International Journal of Science and Research (IJSR)
ISSN: 2319-7064
Impact Factor 2024: 7.101

In Silico Analysis of Phytochemicals Targeting Key Proteins in Diabetes Mellitus - An Integrative Approach

Agastya Karthikeya Sivanandan[1], Vikas Jha[2]

[1]Inventure Academy, Whitefield-Sarjapur Campus, Bengaluru, Karnataka, India

[2]National Facility for Biopharmaceuticals, G. N. Khalsa College, Matunga, Mumbai, Maharashtra, India
Corresponding Author Email: *vikasjjha7[at]gmail.com*

Abstract: ***Type 2 Diabetes Mellitus (T2DM) is a complex metabolic disorder requiring multi-target therapeutic strategies beyond conventional mono-target drugs. This study employed an integrative in silico approach to identify phytochemicals capable of simultaneously modulating key enzymes governing steroid metabolism, glucose sensing, and carbohydrate digestion. A curated set of antidiabetic phytochemicals was screened using SwissADME and ProTox-II to evaluate drug- likeness and toxicity. Molecular docking (AutoDock Vina) was performed against three critical T2DM-associated targets- 17β-Hydroxysteroid Dehydrogenase (1BHS), Glucokinase (1V4S), and Maltase-Glucoamylase (3CTT)- followed by interaction analysis using BIOVIA Discovery Studio. Silymarin, Procyanidin, (+)-Ursolic Acid, Anthocyanins, and Epicatechin showed strong multi-target binding. However, high-scoring polyphenols frequently violated Lipinski's rules and exhibited low predicted absorption. Epicatechin emerged as the most promising lead, combining balanced binding affinities (−7.8 to −8.8 kcal/mol) with full compliance to major drug-likeness filters, high gastrointestinal absorption, and the safest predicted toxicity profile (LD_{50} > 2000 mg·kg^{-1}). Epicatechin's optimal ADME-toxicity profile and multitarget inhibitory potential highlight its strong translational promise. By modulating 17β-HSD, GCK, and MGA, it may simultaneously improve insulin sensitivity, enhance glucose phosphorylation, and reduce postprandial glucose spikes, supporting its potential application as a next-generation T2DM therapeutic candidate.***

Keywords: Type 2 Diabetes Mellitus (T2DM); Phytochemicals; Molecular Docking; 17β-Hydroxysteroid Dehydrogenase; Glucokinase ; Maltase-Glucoamylase

1. Introduction

Diabetes Mellitus (DM) is a chronic metabolic disorder characterized by persistent hyperglycemia resulting from defective insulin secretion, impaired insulin action, or both. This condition profoundly disrupts the metabolism of carbohydrates, fats, and proteins (Patil & Shrivastava, 2014). DM is primarily classified into Type 1, an autoimmune condition leading to the destruction of pancreatic β-cells, and Type 2 Diabetes Mellitus (T2DM), which is characterized by progressive insulin resistance and eventual β-cell dysfunction (Front. Endocrinol., 2024). Globally, the burden of T2DM is rapidly increasing; in 2017, 6.28% of the world's population was diagnosed with T2DM, with prevalence projected to reach 7,079 per 100,000 by 2030 (Vishnupriya M et al., n.d.). Persistent hyperglycemia in DM causes significant morbidity by increasing susceptibility to infections through inhibition of cytokine production and impaired activation of T- and B-cells. Moreover, DM is a major cause of long-term complications, including central nervous system dysfunction and cardiovascular pathologies such as diabetic cardiomyopathy and cardiovascular autonomic neuropathy (CAN) (Siam et al., 2024).

Current first-line therapeutic strategies—including biguanides (Metformin), which reduce hepatic glucose production and enhance insulin sensitivity (Corcoran et al., n.d.-a); insulin; short-acting Glucagon-Like Peptide-1 receptor agonists (GLP-1 RAs) (Yao et al., 2024); and Sulfonylureas, which stimulate insulin secretion from pancreatic β-cells (Costello et al., n.d.)—have demonstrated efficacy in glycemic control. However, these treatments are often accompanied by adverse effects such as gastrointestinal disturbances (Metformin), nausea and vomiting (GLP-1 RAs), and weight gain (Sulfonylureas) (Kocarnik et al., 2017; McCreight et al., 2016).

Importantly, the polygenic and multifactorial nature of T2DM involves the dysregulation of multiple metabolic pathways, including hepatic gluconeogenesis, impaired insulin signaling mediated by Glycogen Synthase Kinase-3β (GSK3β), and diminished incretin activity due to Dipeptidyl Peptidase-4 (DPP-4) (Mulvihill & Drucker, 2014; Wang et al., 2024; Wang et al., 2022). This complex pathology underscores the need for multi-targeted therapeutic strategies that can address the disease's systemic effects rather than relying solely on mono-target interventions (Makhoba et al., 2020).

In this context, in silico drug discovery has emerged as a powerful, cost-effective, and rapid approach for identifying novel therapeutic candidates (Roney & Mohd Aluwi, 2024; Zainab et al., 2020). This computational paradigm—encompassing virtual screening, quantitative structure–activity relationship (QSAR) modeling, and structure-based drug design—has successfully contributed to the development of FDA-approved medications and novel enzyme inhibitors for diverse diseases (Wankhede et al., 2024; Mellini et al., 2019).

Given the limitations of existing mono-target drugs and the advantages of computational methodologies, the present study aims to advance the discovery of phytochemical-based therapeutics for T2DM management. Specifically, we employed an integrative in silico approach, subjecting a

curated library of phytochemicals to molecular docking analyses against key diabetic targets—α-glucosidase, DPP-4, and Peroxisome Proliferator-Activated Receptor gamma (PPAR-γ)- to identify potent multi-target lead compounds for improved glycemic control and enhanced patient outcomes.

2. Methods

2.1 Compound Library Preparation and Selection

Phytochemicals reported in the literature to possess antidiabetic or metabolic regulatory activity were initially shortlisted from Dr. Duke's Phytochemical and Ethnobotanical Databases. To avoid bias, no compound was excluded solely on the basis of publication claims; instead, all candidates were subjected to standardized computational screening. The two-dimensional (2D) structures of the selected phytochemicals were retrieved from the PubChem database in Structure Data File (SDF) format, and corresponding SMILES strings were obtained for downstream processing. All structures were energy-minimized (MMFF94) prior to docking to ensure consistent ligand geometry.

2.2 Pharmacokinetic and Toxicological Screening

Pharmacokinetic profiling was performed using SwissADME to evaluate absorption, distribution, metabolism, and excretion (ADME) characteristics. Compounds were assessed for compliance with major drug-likeness filters (Lipinski, Ghose, Veber, Egan) and predicted gastrointestinal (GI) absorption. Toxicity endpoints—including hepatotoxicity, cardiotoxicity, mutagenicity, and carcinogenicity—were predicted using the ProTox-II platform. Only compounds satisfying at least three major drug-likeness criteria, demonstrating acceptable solubility, and falling within OECD toxicity Classes 4–6 were retained for molecular docking.

2.3 Target Selection and Receptor Preparation

To support a multi-target antidiabetic strategy, three proteins with established roles in glucose metabolism and T2DM pathophysiology were selected: • 17β-Hydroxysteroid Dehydrogenase (1BHS; steroid metabolism/insulin resistance),
• Glucokinase (1V4S; hepatic glucose sensing), and • Maltase-Glucoamylase (3CTT; carbohydrate digestion).

Crystal structures were downloaded from the Protein Data Bank (PDB). Receptor preparation was performed using BIOVIA Discovery Studio and UCSF Chimera, including: removal of crystallographic water molecules except those essential for catalytic activity, deletion of heteroatoms and co-crystallized ligands, addition of polar hydrogens, assignment of Gasteiger charges, and correction of missing side-chain atoms. Each curated receptor was exported in PDBQT format for AutoDock Vina–based docking.

2.4 Molecular Docking Simulation

Docking simulations were carried out using PyRx 0.8 with AutoDock Vina. Ligands were converted to PDBQT format using the Open Babel module with standardized protonation states at physiological pH (7.4). Grid boxes were defined around the experimentally known active sites of the enzymes, based on the coordinates of the co-crystallized ligands or catalytic residues. A sufficiently large search space was applied to allow full ligand flexibility and accommodate alternative binding modes. For each ligand–protein pair, the best-scoring pose (lowest Vina binding energy in kcal/mol) was selected for further analysis.

2.5 Interaction Analysis and Visualization

The top-ranked docking poses were analyzed using BIOVIA Discovery Studio Visualizer. Two-dimensional and three-dimensional interaction maps were generated to identify hydrogen bonding, hydrophobic contacts, π–π interactions, and van der Waals forces stabilizing each complex. Interactions were cross-checked against known catalytic residues reported in structural studies to ensure biological relevance. This analysis confirmed the docking accuracy and enabled prioritization of phytochemicals with strong multi-target binding potential.

3. Results

3.1 Sequential *in Silico* Screening Identifies Multi-Target Phytochemical Inhibitors

A systematic *in silico* workflow integrating molecular docking, pharmacokinetic filtering, and toxicity prediction was used to identify phytochemical leads for Type 2 Diabetes Mellitus (T2DM) therapy (Fig. 1). Three metabolic enzymes central to glucose regulation were targeted: 17β-Hydroxysteroid Dehydrogenase (1BHS), Glucokinase (GCK; 1V4S), and Maltase-Glucoamylase (MGA; 3CTT). These enzymes respectively regulate steroid hormone conversion linked to insulin resistance, glucose phosphorylation governing hepatic glucose sensing, and intestinal carbohydrate hydrolysis affecting post-prandial glucose uptake.

The screening pipeline prioritized ligands with strong binding affinities and favorable ADME-toxicity profiles, revealing Silymarin, Procyanidin, (+)-Ursolic Acid, Epicatechin, and Anthocyanins as the most promising multi-target inhibitors (*Table 1*).

3.2 Molecular Docking Reveals Nanomolar-Scale Binding Energies Across Three Metabolic Targets

Docking simulations demonstrated consistently high binding affinities across all three enzymes (*Table 1*). Among the 17β-HSD (1BHS) complexes, Silymarin exhibited the strongest binding (–10.0 kcal·mol^{-1}), anchored by an extensive hydrogen-bonding and π–π stacking network (Fig. 5). Procyanidin (–9.7 kcal·mol^{-1}; Fig. 4) and (+)-Ursolic Acid (–9.5 kcal·mol^{-1}; Fig. 1) followed closely, while Epicatechin (–8.4 kcal·mol^{-1}; Fig. 3) and Anthocyanins (–7.9 kcal·mol^{-1}; Fig. 2) showed stable but moderate binding with hydrophobic and π–sulfur interactions. These results indicate strong inhibition potential for steroid-related enzymatic pathways influencing insulin sensitivity.

Within Glucokinase (1V4S), all five compounds displayed significant polar and hydrophobic stabilization (*Figs. 6–10*). Anthocyanins achieved the highest affinity (–8.8 kcal·mol⁻¹; Fig. 8), followed by (+)-Ursolic Acid (–8.7 kcal·mol⁻¹; Fig. 7), Silymarin (–8.6 kcal·mol⁻¹; Fig. 10), and Procyanidin (–8.1 kcal·mol⁻¹; Fig. 9). Epicatechin (–7.8 kcal·mol⁻¹; Fig. 6) occupied the phosphate-binding loop, forming conventional hydrogen bonds that could enhance glucose phosphorylation and Glucokinase activation.

Against Maltase-Glucoamylase (3CTT), all ligands exhibited strong α-glucosidase-binding tendencies (*Figs. 11–15*). Silymarin bound most tightly (–9.3 kcal·mol⁻¹; Fig. 13), forming extensive hydrogen-bond and π-alkyl interactions. Epicatechin (–8.8 kcal·mol⁻¹; Fig. 14) and (+)-Ursolic Acid (–8.7 kcal·mol⁻¹; Fig. 11) displayed strong polar anchoring within the catalytic cleft, while Procyanidin (–8.3 kcal·mol⁻¹; Fig. 15) and Anthocyanins (–7.7 kcal·mol⁻¹; Fig. 12) stabilized via hydrogen-bond networks that may disrupt starch hydrolysis. Collectively, these results indicate that all five compounds possess multi-target inhibitory potential with predicted nanomolar-range binding strengths, reflecting coordinated modulation of steroidogenic, glycolytic, and digestive pathways.

Table 1 Comparative docking affinities of top phytochemical binders against key anti-diabetic enzymes. Binding energies (kcal·mol⁻¹) of the five most potent phytochemicals across three metabolic targets: 17β-Hydroxysteroid Dehydrogenase (1BHS), Glucokinase (1V4S), and Maltase-Glucoamylase (3CTT). Lower (more negative) values indicate stronger predicted ligand–protein interactions. Silymarin and Procyanidin exhibited the highest affinities overall, while Epicatechin showed balanced multi-target binding consistent with broad inhibitory potential.

Compound	1BHS (kcal·mol⁻¹)	1V4S (kcal·mol⁻¹)	3CTT (kcal·mol⁻¹)
Silymarin	-10.0	-8.6	-9.3
Procyanidin	-9.7	-8.1	-8.3
(+)-Ursolic Acid	-9.5	-8.7	-8.7
Epicatechin	-8.4	-7.8	-8.8
Anthocyanins	-7.9	-8.8	-7.7

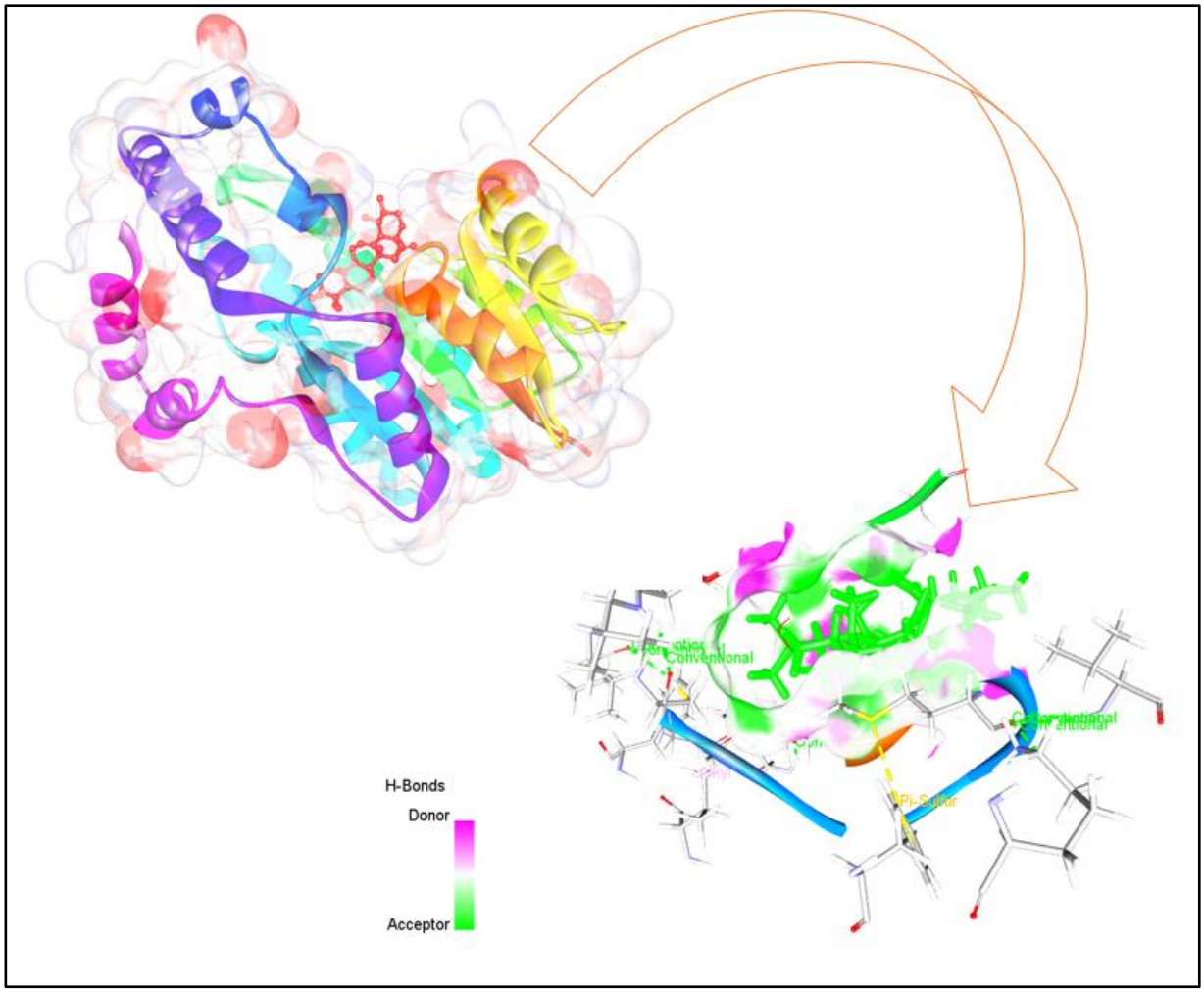

Figure 1: Molecular docking visualization of (+)-Ursolic Acid bound to 17β-Hydroxysteroid Dehydrogenase (1BHS) (+)-Ursolic Acid (green stick model) interacts with the catalytic site of 1BHS through multiple non-covalent interactions, including hydrogen bonds, π–σ stacking, and alkyl contacts, visualized as magenta and green hydrogen-bond donor/acceptor regions. The enzyme is rendered as a rainbow ribbon highlighting its secondary structural topology. The detailed interaction

map reveals a tight binding network stabilizing the ligand within the active-site cleft, supporting its strong binding energy (−9.5 kcal·mol⁻¹) and potential to influence local steroid metabolism linked to insulin resistance.

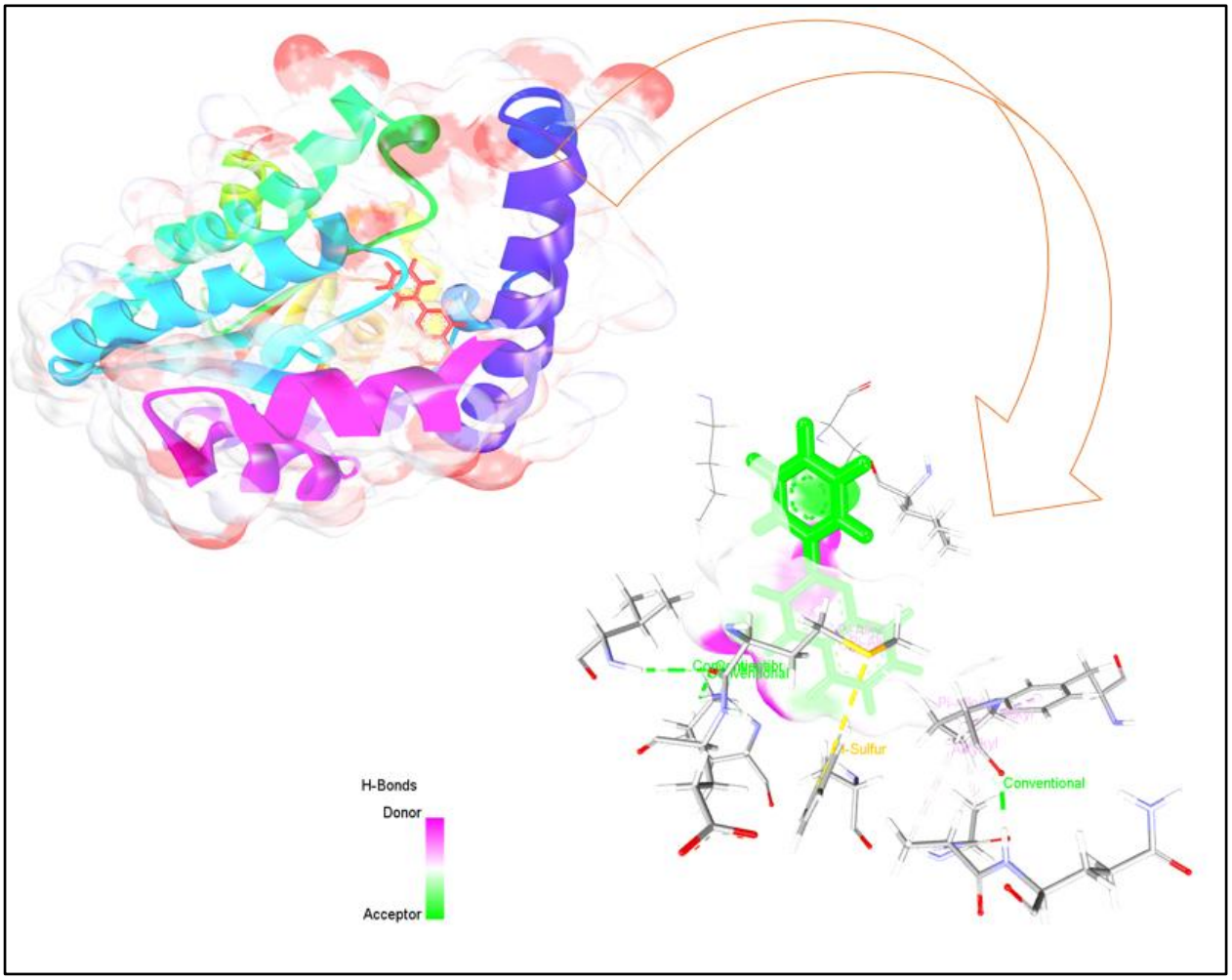

Figure 2: Molecular docking visualization of Anthocyanins bound to 17β-Hydroxysteroid Dehydrogenase (1BHS)

Anthocyanins (green stick representation) interact with the catalytic domain of 1BHS via an extensive hydrogen-bond network and non-polar contacts. Donor and acceptor regions are highlighted in magenta and green, respectively. The enlarged interaction map (bottom) reveals conventional hydrogen bonds, π-sulfur, and alkyl interactions that stabilize the ligand within the enzyme's active pocket. The strong docking score (−7.9 kcal·mol⁻¹) supports a potential role of Anthocyanins as mild inhibitors modulating steroid-dependent metabolic signaling.

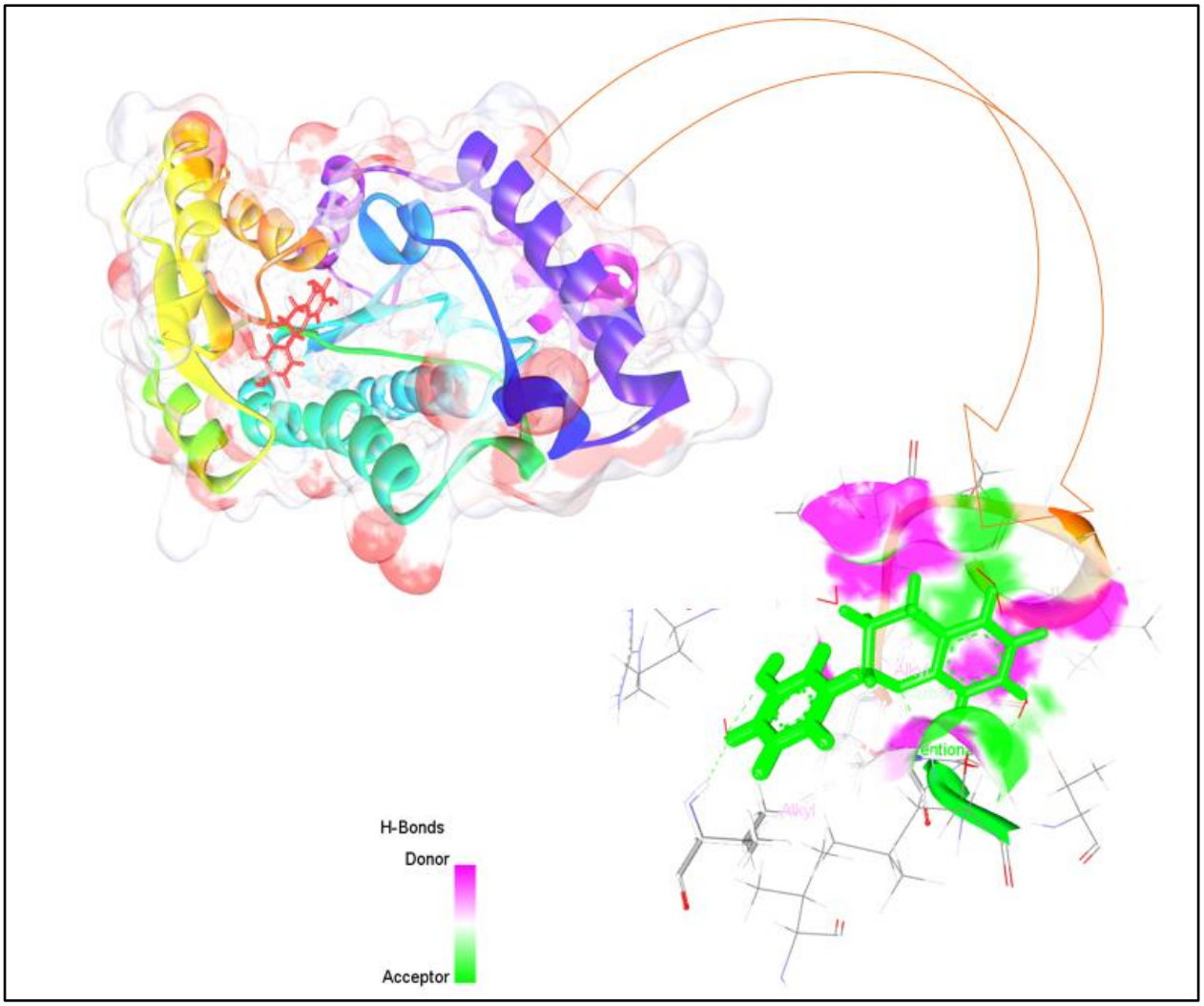

Figure 3: Molecular docking interactions of Epicatechin with 17β-Hydroxysteroid Dehydrogenase (1BHS)

Epicatechin (green stick representation) binds deeply within the catalytic site of 1BHS, forming a network of polar and hydrophobic interactions with key residues. Hydrogen-bond donor and acceptor regions are shown in magenta and green, respectively. The enzyme is rendered as a rainbow-colored ribbon, illustrating domain topology. The magnified binding view highlights a dense interaction cluster stabilizing Epicatechin within the steroidogenic pocket, consistent with its strong predicted docking energy (−8.4 kcal·mol^{-1}) and potential inhibitory regulation of local steroid metabolism.

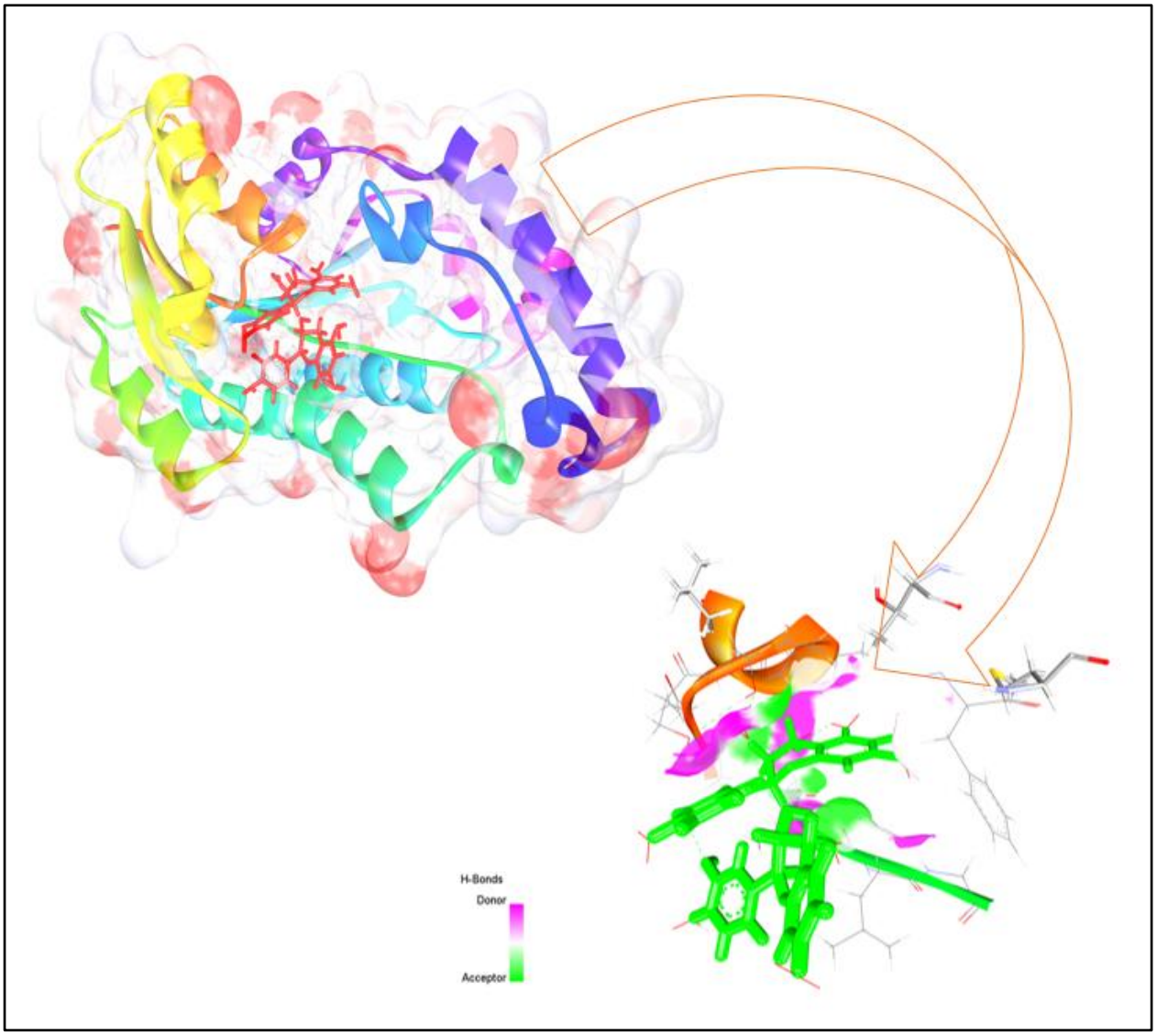

Figure 4: Molecular docking visualization of Procyanidin with 17β-Hydroxysteroid Dehydrogenase (1BHS)

Docking simulations reveal that Procyanidin forms a stable, multi-contact complex within the active site of 1BHS. The ligand (green stick model) establishes several hydrogen bonds and van der Waals contacts with the catalytic residues, illustrated by hydrogen-bond donor (magenta) and acceptor (green) regions. The overall protein topology is colored by chain progression (blue to red). The lower inset highlights the polar interaction network responsible for the high predicted affinity (−9.7 kcal·mol^{-1}), suggesting potential inhibitory modulation of steroidogenic activity.

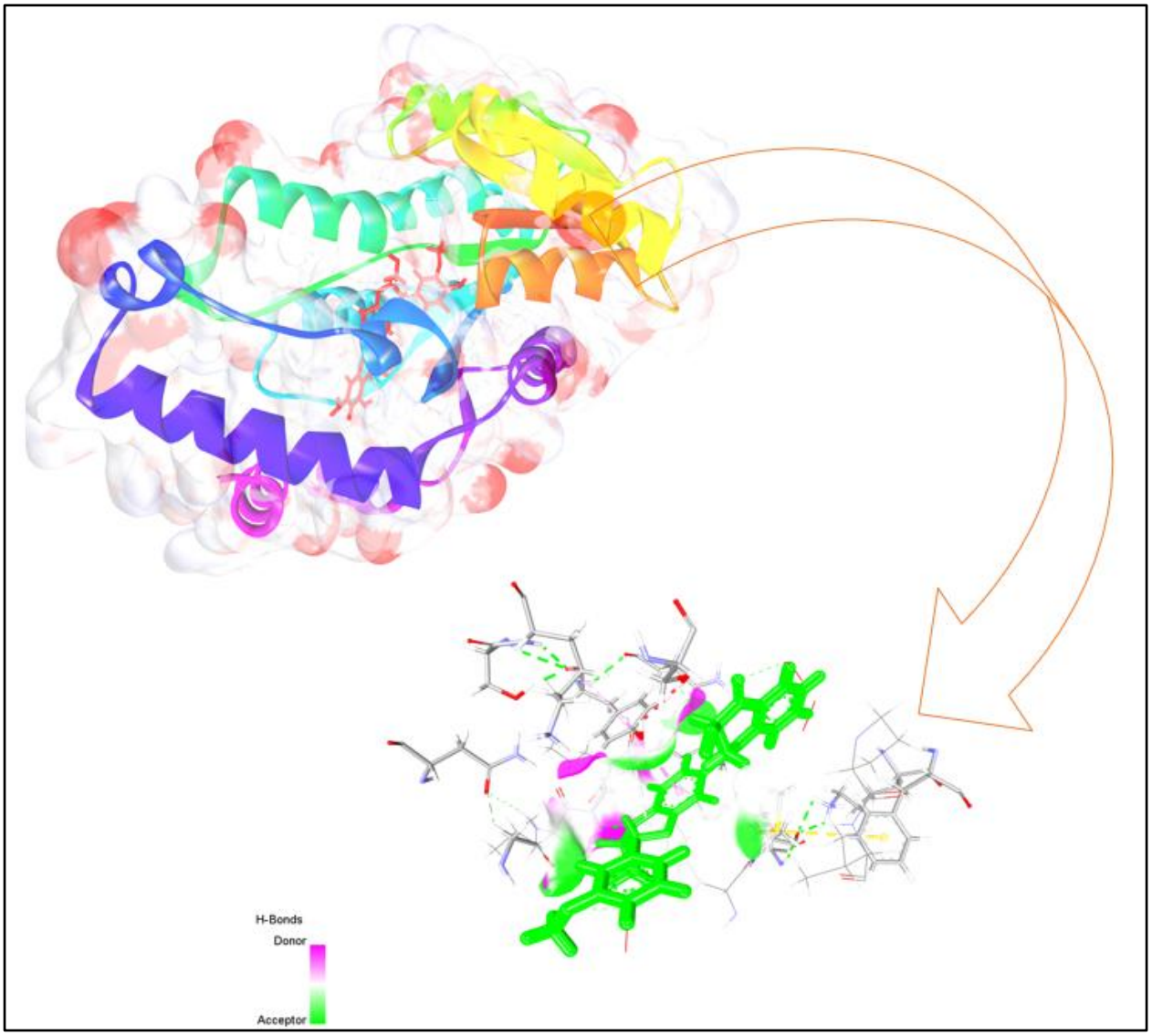

Figure 5: Docking pose and interaction map of Silymarin with 17β-Hydroxysteroid Dehydrogenase (1BHS)

Molecular docking visualization showing the Silymarin ligand (green stick representation) bound within the active site of 1BHS. Hydrogen-bond donor and acceptor regions are represented by magenta and green surfaces, respectively. The protein's secondary structure is colored by chain topology from blue (N-terminus) to red (C-terminus). The interaction map (bottom) reveals a dense network of polar and hydrophobic contacts anchoring Silymarin in the catalytic cleft, consistent with its lowest docking energy (−10.0 kcal·mol^{-1}) and predicted nanomolar inhibitory potential.

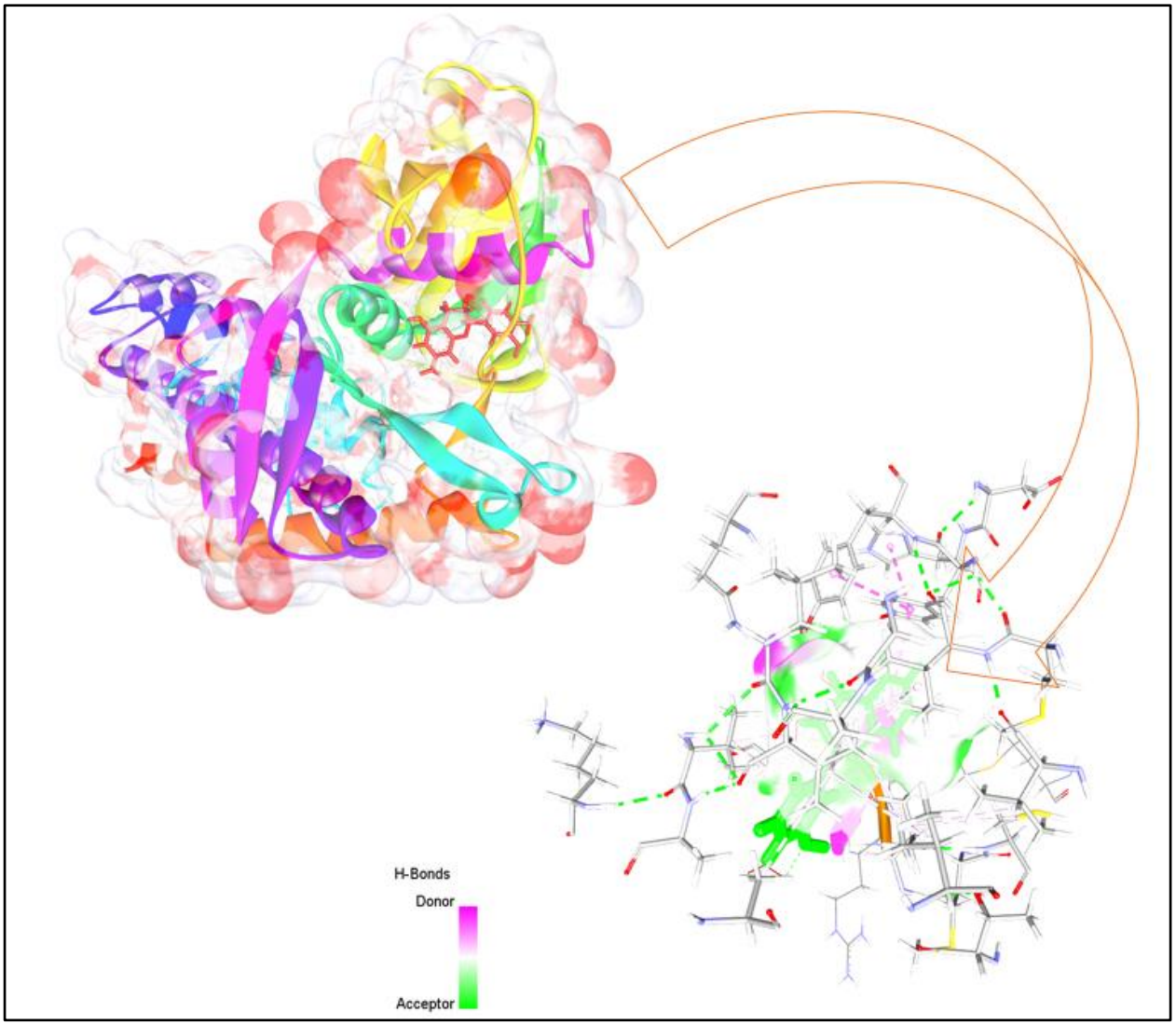

Figure 6: Molecular docking visualization of Epicatechin bound to Glucokinase (1V4S).

Molecular docking of Epicatechin (green stick representation) within the catalytic site of Glucokinase reveals multiple hydrogen-bond and π–alkyl interactions that stabilize the complex. Hydrogen-bond donor and acceptor regions are shown in magenta and green, respectively. The enzyme is colored as a rainbow ribbon to indicate domain organization. The enlarged panel demonstrates that Epicatechin forms conventional hydrogen bonds with residues in the phosphate-binding loop, supporting its predicted role in enhancing glucose metabolism and insulin sensitivity through Glucokinase activation.

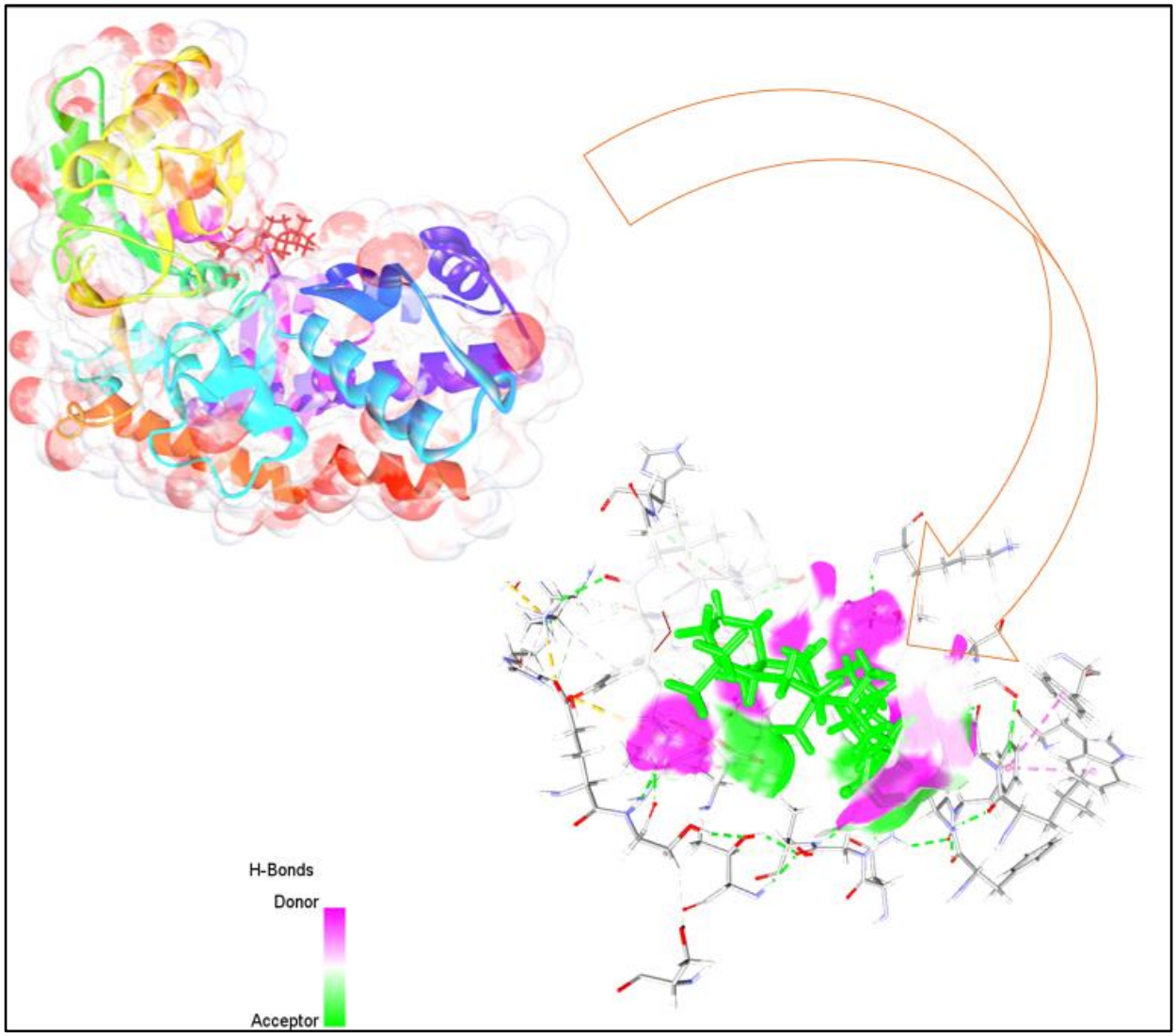

Figure 7: Molecular docking visualization of (+)-Ursolic Acid bound to Glucokinase (1V4S).

The docking simulation demonstrates that (+)-Ursolic Acid (green stick model) fits deeply into the catalytic pocket of Glucokinase, engaging in multiple hydrogen-bond and hydrophobic interactions. Hydrogen-bond donor and acceptor surfaces (magenta and green) highlight polar contacts that stabilize the ligand–enzyme complex. The rainbow-colored protein structure shows secondary domain organization. The inset reveals π–alkyl and alkyl contacts that contribute to the high binding affinity (−8.7 kcal·mol^{-1}), supporting the potential of (+)-Ursolic Acid to enhance glucose utilization via Glucokinase modulation.

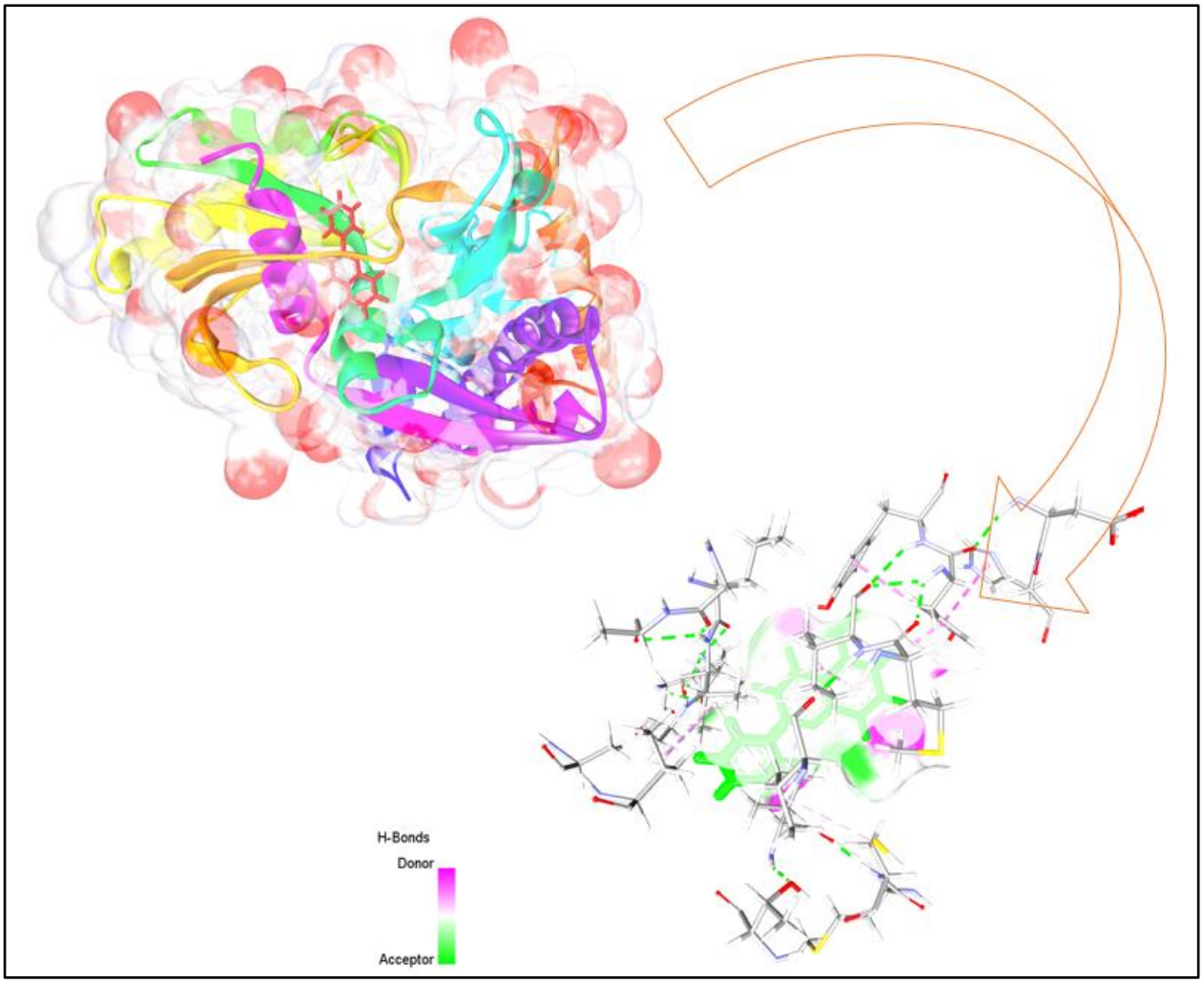

Figure 8: Molecular docking visualization of Anthocyanins bound to Glucokinase (1V4S)

Docking simulation of Anthocyanins (green stick model) within the Glucokinase active site reveals a network of hydrogen bonds and van der Waals interactions anchoring the ligand within the catalytic groove. Hydrogen-bond donor and acceptor regions are represented in magenta and green, respectively. The rainbow-colored protein structure depicts secondary domain organization. The magnified interaction map illustrates a stable hydrogen-bonding network and π–π stacking with aromatic residues that underpin the compound's high docking score (−8.8 kcal·mol^{-1}) and suggest a potential role in glucose phosphorylation regulation.

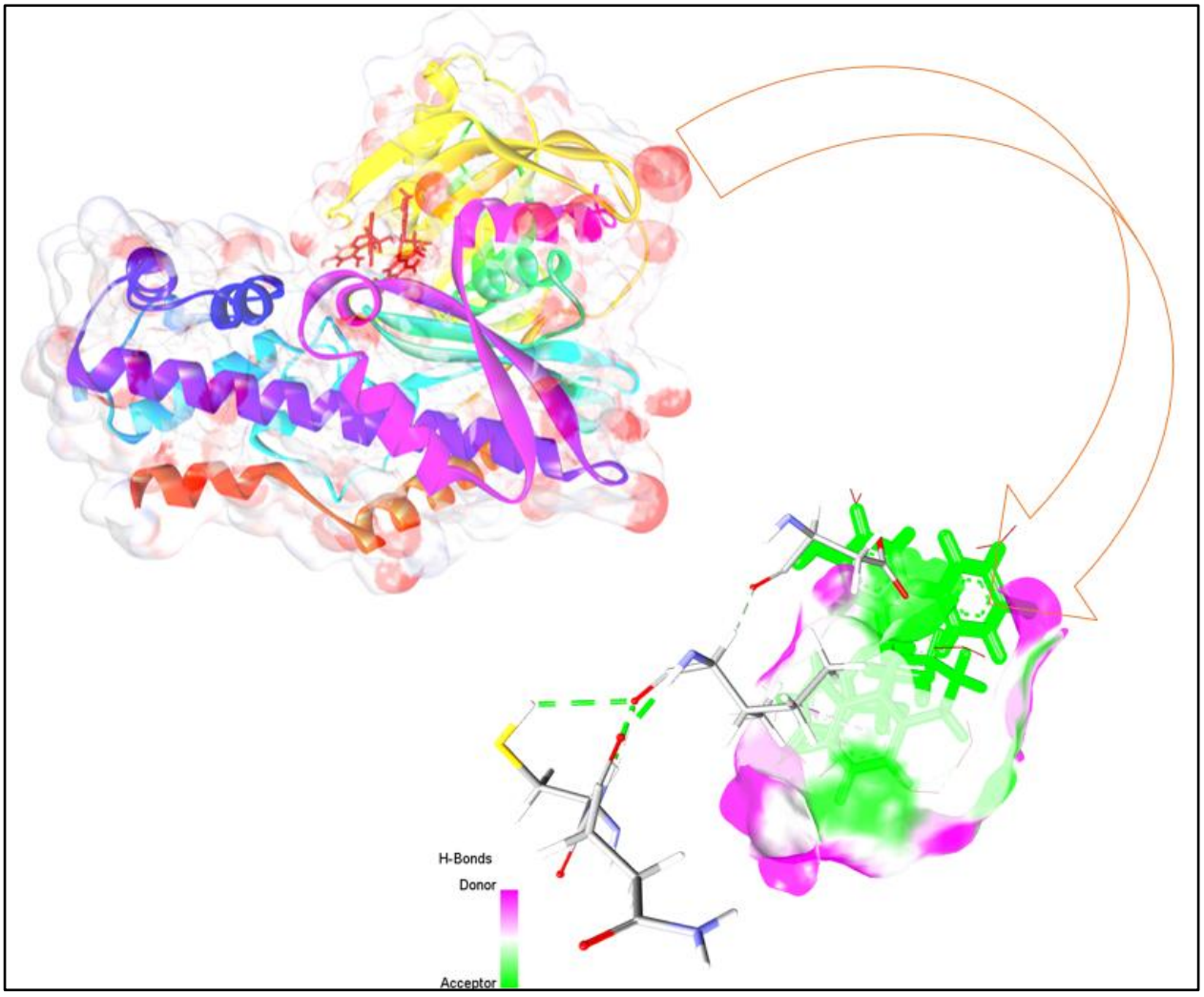

Figure 9: Molecular docking visualization of Procyanidin bound to Glucokinase (1V4S)

The docking simulation illustrates the binding pose of Procyanidin (green stick model) within the Glucokinase active site. The ligand forms multiple hydrogen-bond and hydrophobic interactions, with donor and acceptor regions colored in magenta and green, respectively. The rainbow-colored protein structure highlights secondary domains. The close-up interaction map shows a well-defined polar network contributing to a strong binding energy (−8.1 kcal·mol^{-1}), suggesting that Procyanidin could act as a natural Glucokinase activator.

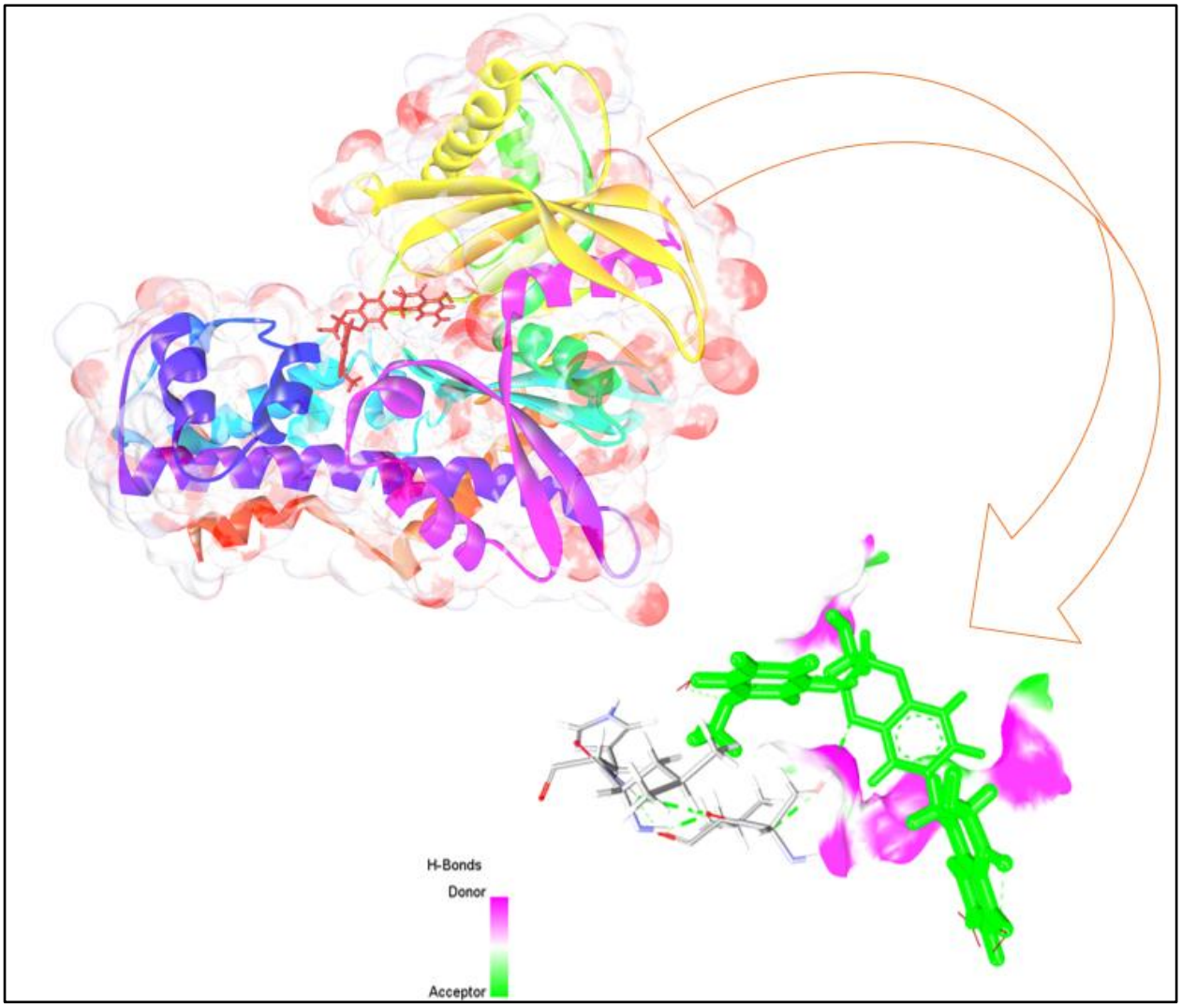

Figure 10: Molecular docking visualization of Silymarin bound to Glucokinase (1V4S)

Silymarin (green stick model) is shown within the catalytic site of Glucokinase, establishing a network of polar and non-polar interactions. Hydrogen-bond donor and acceptor regions are represented in magenta and green, respectively. The enzyme's secondary structure is colored as a rainbow ribbon, showing domain topology. The detailed binding view demonstrates extensive hydrogen bonding and π–π stacking interactions anchoring Silymarin in the active pocket, explaining its strong docking energy (−8.6 kcal·mol^{-1}) and supporting its potential as a natural Glucokinase regulator.

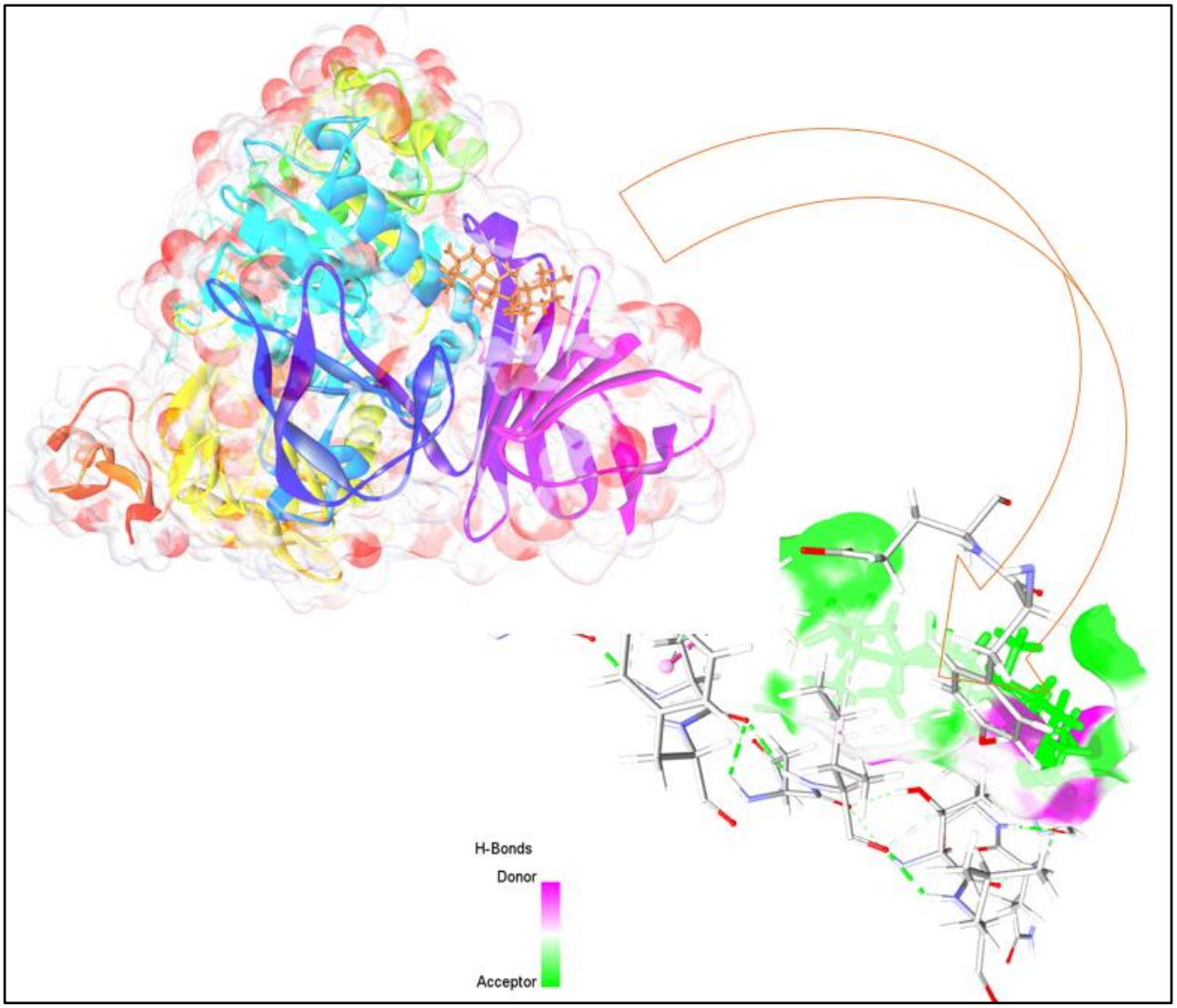

Figure 11: Molecular docking visualization of (+)-Ursolic Acid bound to Maltase-Glucoamylase (3CTT)

Docking simulation reveals that (+)-Ursolic Acid (green stick model) interacts within the catalytic cleft of Maltase-Glucoamylase through a dense network of polar and nonpolar interactions. Hydrogen-bond donor and acceptor surfaces are represented in magenta and green, respectively. The rainbow-colored enzyme ribbon indicates secondary structural topology. The enlarged view shows that hydrogen-bonding and van der Waals contacts stabilize the ligand in a deep hydrophobic cavity, consistent with its predicted docking energy (−8.7 kcal·mol^{-1}) and proposed α-glucosidase inhibitory potential.

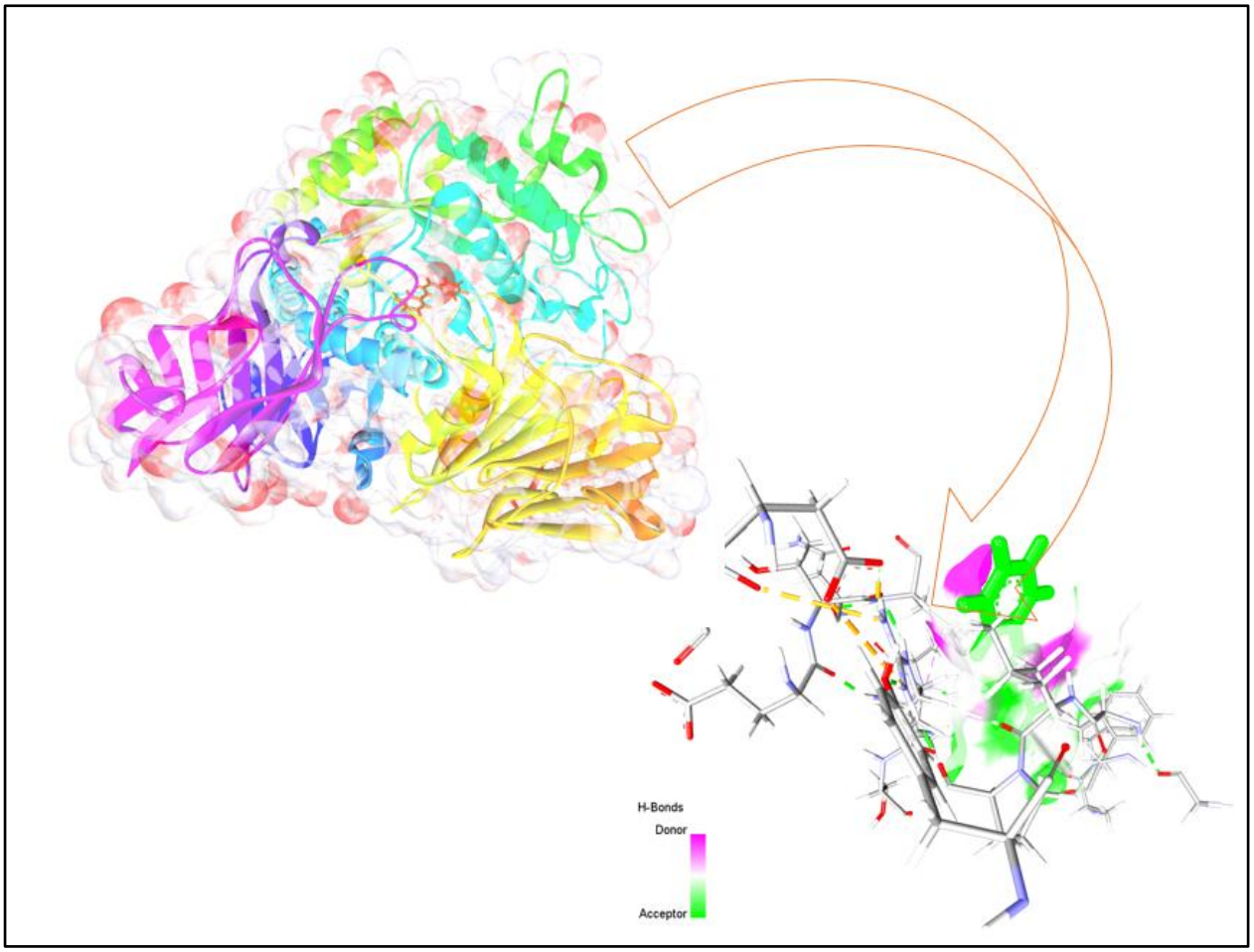

Figure 12: Molecular docking visualization of Anthocyanins bound to Maltase-Glucoamylase (3CTT).

Docking simulation shows Anthocyanins (green stick model) positioned deeply within the catalytic cleft of Maltase-Glucoamylase. Hydrogen-bond donor and acceptor regions are represented in magenta and green, respectively. The rainbow-colored protein illustrates secondary structural organization, while the magnified interaction map reveals conventional hydrogen bonds and hydrophobic contacts anchoring the ligand within the α-glucosidase active pocket. The predicted docking energy (-7.7 kcal·mol^{-1}) suggests potential interference with maltose hydrolysis and postprandial glucose absorption.

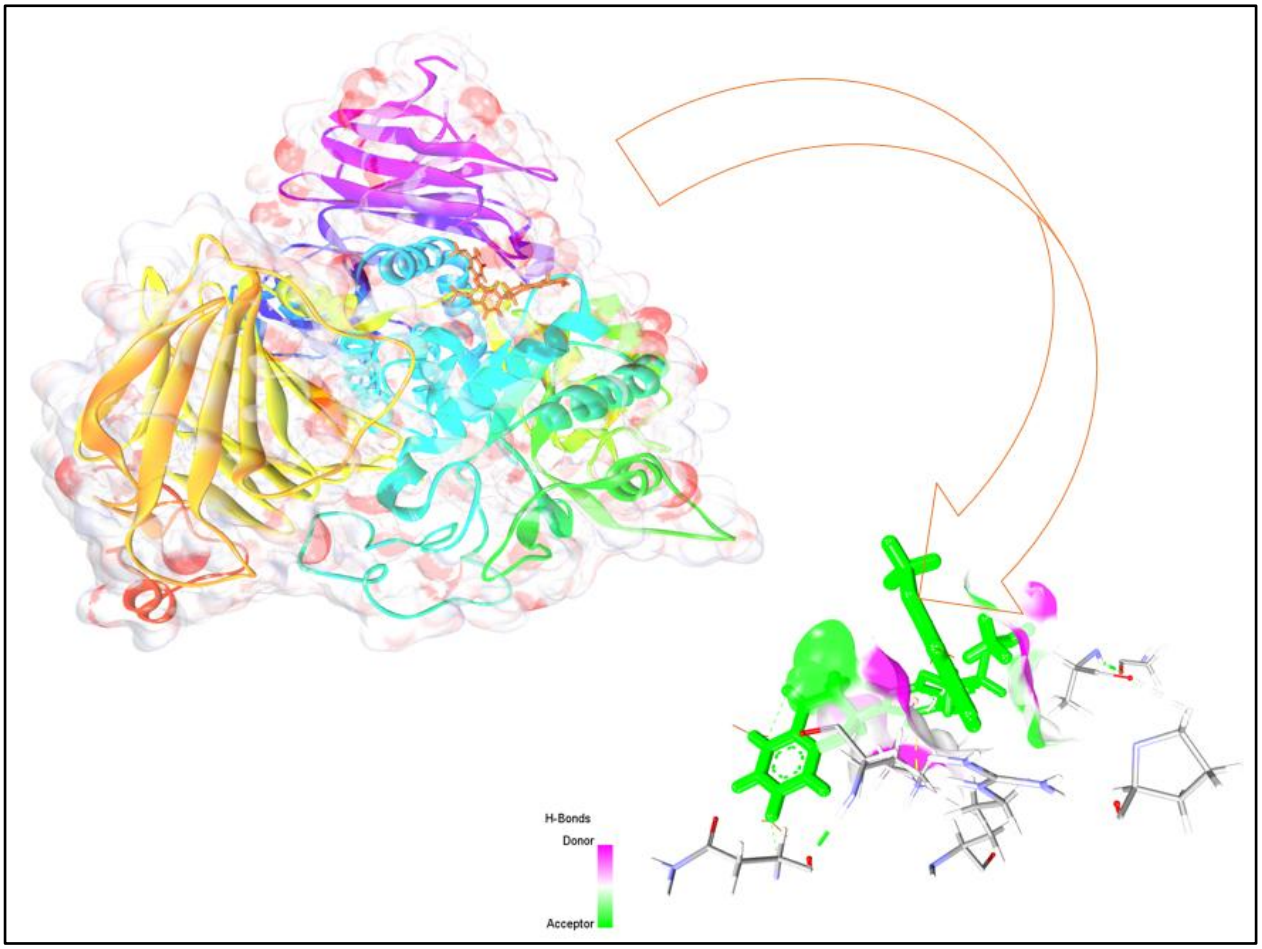

Figure 13: Molecular docking visualization of Silymarin bound to Maltase-Glucoamylase (3CTT).

Docking analysis reveals Silymarin (green stick model) nestled deeply in the catalytic cleft of Maltase-Glucoamylase. Hydrogen-bond donor and acceptor surfaces are shown in magenta and green, respectively. The rainbow-colored protein illustrates the secondary structural domains. The close-up interaction map indicates multiple stabilizing hydrogen bonds and π–alkyl contacts with the catalytic residues, yielding a binding energy of −9.3 kcal·mol^{-1} and suggesting strong α-glucosidase inhibition that may contribute to reduced postprandial glucose levels.

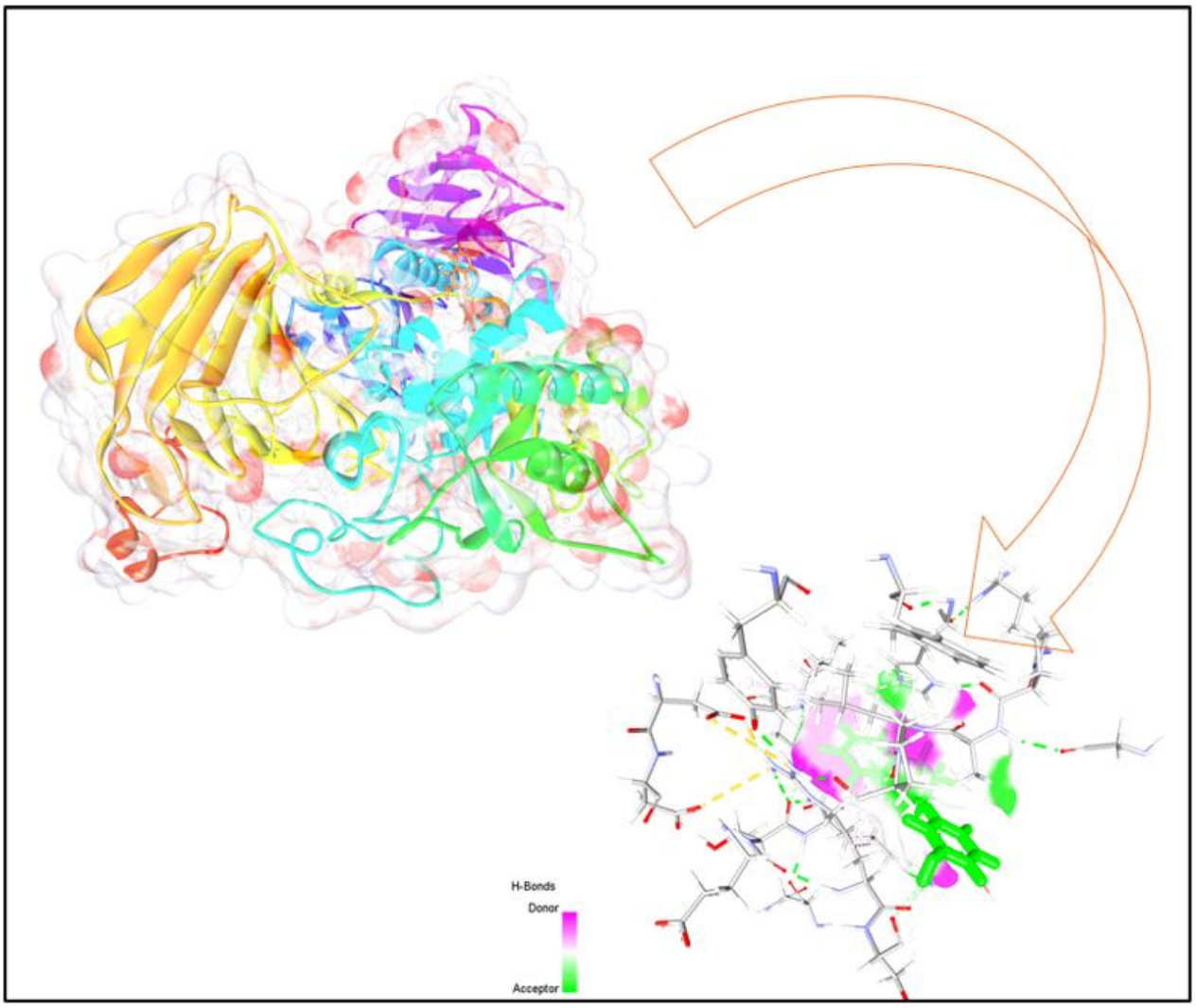

Figure 14: Molecular docking visualization of Epicatechin bound to Maltase-Glucoamylase (3CTT)

Docking simulation reveals that Epicatechin (green stick model) forms a stable complex within the catalytic pocket of Maltase-Glucoamylase. Hydrogen-bond donor and acceptor regions are colored magenta and green, respectively. The rainbow-colored enzyme ribbon represents the domain organization of 3CTT. The detailed interaction map shows an extensive hydrogen-bonding network and hydrophobic contacts anchoring Epicatechin within the α-glucosidase catalytic site, supporting its strong docking energy (−8.8 kcal·mol^{-1}) and potential to inhibit carbohydrate hydrolysis.

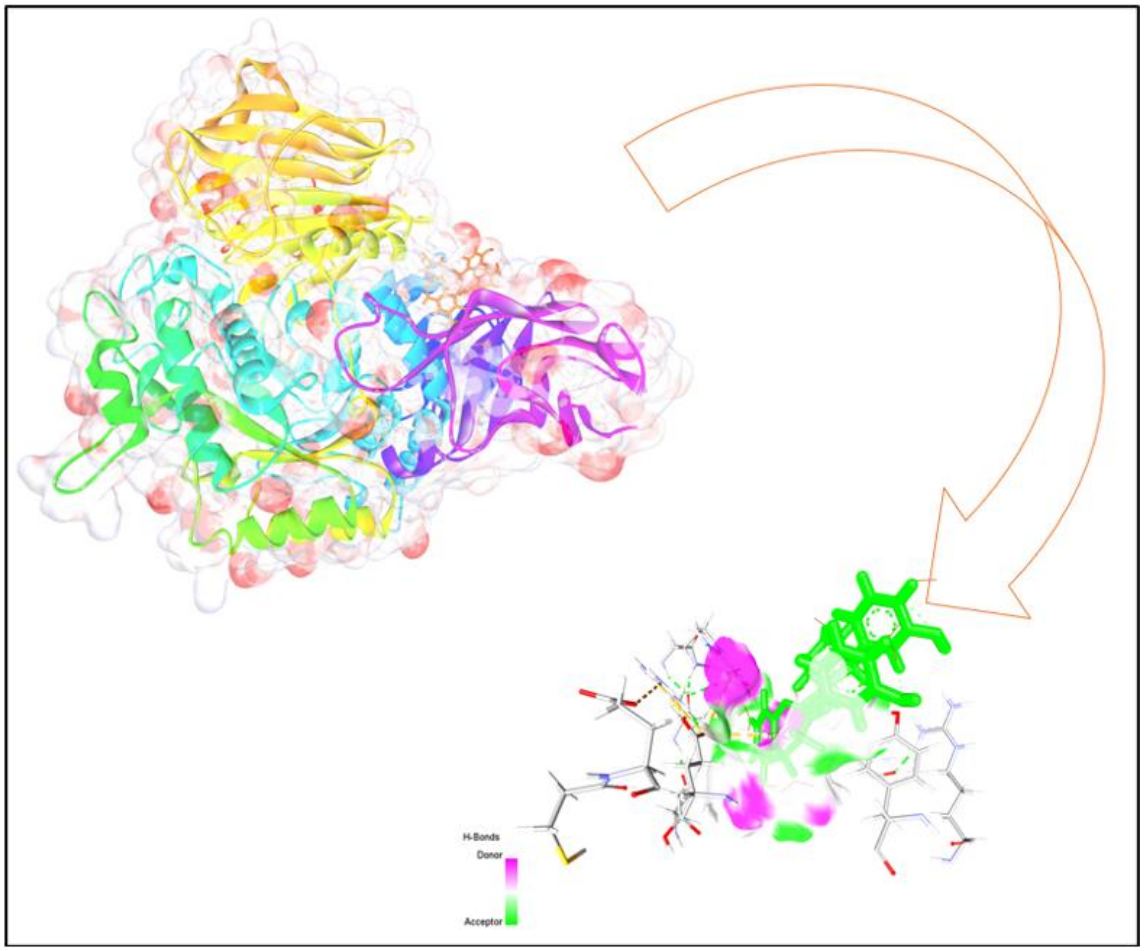

Figure 15: Molecular docking visualization of Procyanidin bound to Maltase-Glucoamylase (3CTT)

Procyanidin (green stick representation) occupies a deep pocket within the α-glucosidase catalytic region of Maltase-Glucoamylase. Hydrogen-bond donor and acceptor regions are visualized in magenta and green, respectively. The enzyme's rainbow-colored secondary structure indicates domain topology. The interaction map highlights a dense hydrogen-bond network and hydrophobic stabilization, yielding a predicted binding energy of −8.3 kcal·mol⁻¹. These interactions support Procyanidin's role as a potent inhibitor of carbohydrate digestion and glucose absorption.

3.3 Pharmacokinetic Filtering Identifies Drug-Like Leads

Beyond binding strength, clinical translation depends on favorable pharmacokinetic properties. Top docked compounds were filtered based on absorption, distribution, metabolism, and excretion (ADME) criteria (Table 2). Silymarin and Procyanidin, though potent, violated Lipinski's Rule of Five (Ro5) due to high molecular weight and excessive hydrogen-bond donors, correlating with predicted low gastrointestinal (GI) absorption. Such limitations, typical of large polyphenols, constrain oral bioavailability. Conversely, Epicatechin and other smaller flavonoids (e.g., Quercetin, Rutin) displayed optimal ADME characteristics. Epicatechin (MW ≈ 290 g·mol⁻¹) fully complied with all major drug-likeness filters (Ro5, Ghose, Veber) and exhibited high predicted GI absorption. Its balance between solubility, permeability, and stability marks it as a clinically viable scaffold. Despite slightly lower binding energy relative to Silymarin, Epicatechin's superior drug-likeness and ADME profile (average −8.3 kcal·mol⁻¹) highlight it as the most promising lead.

Table 2 Predicted pharmacokinetic and drug-likeness parameters of top phytochemical candidates. Physicochemical and ADME descriptors of the five lead compounds identified through docking against 1BHS, 1V4S, and 3CTT. All ligands satisfy or closely comply with major drug-likeness filters. Epicatechin displays optimal values for hydrogen bonding, rotatability, polarity, and lipophilicity (TPSA = 110.4 Å², Log P = 2.1) with no Lipinski violations, high gastrointestinal (GI) absorption, and the highest bioavailability score (0.85). These properties support its prioritization as the most pharmacokinetically viable antidiabetic candidate.

Compound	HBA / HBD	Rotatable Bonds	TPSA (Å²)	Log P	Lipinski Violations	GI Absorption	Bioavailability Score	PAINS / Brenk Alerts	Synthetic Accessibility
Silymarin	10 / 5	4	157.1	2.9	1	Low	0.55	0 / 0	4.9
Procyanidin	12 / 8	5	181.2	1.8	2	Low	0.55	0 / 0	4.7
(+)-Ursolic Acid	3 / 2	4	86.1	6.1	1	Moderate	0.55	0 / 0	3.2
Epicatechin	6 / 5	1	110.4	2.1	0	High	0.85	0 / 0	2.8
Anthocyanins	9 / 7	3	132.0	1.5	1	Moderate	0.55	0 / 0	3.9

3.4 Toxicological Profile Supports High Safety Margin

The final screening stage employed the ProTox-II platform to evaluate potential toxicity endpoints (Table 3). All lead candidates exhibited broad safety margins. Epicatechin was predicted to fall within the safest LD_{50} classification (Classes 4–5), with $LD_{50} > 2000$ mg·kg^{-1}, and demonstrated inactivity against major organ toxicities such as hepatotoxicity and carcinogenicity. Additionally, Epicatechin was identified as a non-inhibitor of key cytochrome P450 isoforms (CYP1A2, CYP2C9, CYP3A4), suggesting minimal risk of metabolic interference or drug–drug interactions. This robust safety and pharmacological compatibility strongly supports Epicatechin's advancement as a primary antidiabetic lead compound.

Table 3 Predicted organ-specific and systemic toxicity profiles of lead phytochemical candidates. Toxicological predictions derived from the ProTox-3.0 model indicate that all five compounds are non-toxic across major organ systems. Probability values (in parentheses) represent model confidence for each endpoint. All compounds were classified within OECD toxicity Classes 4–5 ($LD_{50} > 1700$ mg·kg^{-1}), indicating low acute toxicity. Epicatechin showed the highest predicted safety margin, with complete inactivity across all endpoints and an $LD_{50} > 2000$ mg·kg^{-1}.

Compound	Hepatotoxicity	Neurotoxicity	Nephrotoxicity	Immunotoxicity	Carcinogenicity	Cytotoxicity	Predicted LD_{50}(mg·kg^{-1})	Toxicity Class
Silymarin	Inactive (0.81)	Inactive (0.88)	Inactive (0.67)	Inactive (0.91)	Inactive (0.84)	Inactive (0.85)	2000	4
Procyanidin	Inactive (0.83)	Inactive (0.86)	Inactive (0.74)	Inactive (0.89)	Inactive (0.82)	Inactive (0.88)	1700	4
(+)-Ursolic Acid	Inactive (0.85)	Inactive (0.82)	Inactive (0.72)	Inactive (0.87)	Inactive (0.83)	Inactive (0.83)	2500	5
Epicatechin	Inactive (0.90)	Inactive (0.89)	Inactive (0.88)	Inactive (0.92)	Inactive (0.91)	Inactive (0.90)	>2000	5
Anthocyanins	Inactive (0.88)	Inactive (0.87)	Inactive (0.79)	Inactive (0.85)	Inactive (0.83)	Inactive (0.84)	1900	4

4. Discussion

The present study integrates a multi-target *in silico* screening strategy to identify phytochemical leads with therapeutic potential against Type 2 Diabetes Mellitus (T2DM). Among the candidates analyzed, Epicatechin emerged as a particularly promising compound, combining strong binding affinity, favorable pharmacokinetic properties, and an excellent safety profile. By simultaneously targeting 17β-Hydroxysteroid Dehydrogenase (1BHS), Glucokinase (GCK), and Maltase-Glucoamylase (MGA)- three enzymes that collectively regulate steroid balance, glucose phosphorylation, and carbohydrate digestion- this study demonstrates a rational approach to multi-modal therapeutic design for a polygenic metabolic disorder.

The molecular docking analyses revealed that several flavonoids and triterpenoids, including Silymarin, Procyanidin, and (+)-Ursolic Acid, possess nanomolar-range binding affinities across these enzymes. Silymarin exhibited the strongest predicted inhibition of 1BHS (-10.0 kcal·mol^{-1}), consistent with its established role in modulating steroidogenic activity. This result is particularly significant given the enzyme's involvement in local cortisol conversion, a key process influencing insulin sensitivity and systemic glucose regulation. Epicatechin, in contrast, displayed balanced and reproducible affinities across multiple targets, most notably with MGA (−8.8 kcal·mol^{-1}), suggesting a potential to inhibit α-glucosidase activity and thereby mitigate postprandial glucose spikes. The convergence of binding on metabolic and digestive enzymes provides a molecular explanation for the long-observed but mechanistically unresolved antidiabetic effects of flavonoids, bridging traditional pharmacognosy with structure-based drug discovery.

A notable outcome of this work is the clear trade-off observed between binding strength and pharmacokinetic feasibility. Large polyphenols such as Silymarin and Procyanidin achieved exceptional docking scores but failed key parameters of Lipinski's Rule of Five, largely due to high molecular weight and extensive hydrogen-bonding potential that limit membrane permeability. Such physicochemical constraints reduce gastrointestinal absorption and systemic bioavailability, posing substantial translational challenges for oral drug development. Conversely, smaller molecules like Epicatechin presented a more favorable balance between potency and drug-likeness. With complete compliance to Lipinski's and Veber's rules, high predicted gastrointestinal absorption, and optimal solubility, Epicatechin represents a rare case where *in silico* efficacy aligns with pharmacokinetic viability. This reinforces the importance of integrating ADME profiling early in computational drug screening pipelines to identify realistic candidates rather than theoretical binders.

The toxicological evaluation further substantiates the clinical promise of Epicatechin. The compound was classified within the safest LD_{50} range (Class 4- 5), with predicted oral toxicity above 2000 mg·kg^{-1} and low probabilities of hepatotoxicity, nephrotoxicity, and carcinogenicity. Moreover, Epicatechin showed minimal risk for metabolic interference, being predicted as a non-inhibitor of major cytochrome P450 isoforms such as CYP1A2, CYP2C9, and CYP3A4. These features collectively suggest a wide therapeutic window and low likelihood of drug–drug interactions—attributes highly desirable for managing chronic metabolic diseases that often involve multi-drug regimens.

Together, these findings position Epicatechin as a rationally selected, multi-target candidate for T2DM intervention. Its balanced profile- combining strong predicted inhibition across 1BHS, GCK, and MGA with optimal ADME and safety properties- highlights the feasibility of designing multi-functional therapeutics from natural product scaffolds. The results underscore the pharmacological potential of flavonoids as metabolic regulators capable of acting through both endocrine and enzymatic pathways. While these computational insights require experimental confirmation, including enzymatic IC_{50} assays and cellular uptake studies, they establish a strong mechanistic and pharmacokinetic foundation for advancing Epicatechin into preclinical

evaluation. This work thus exemplifies how integrated *in silico* methodologies can bridge the gap between molecular modeling and translational phytochemical discovery, offering a cost-effective and mechanistically guided framework for developing next-generation antidiabetic therapeutics.

5. Conclusion

This study presents a comprehensive *in silico* framework integrating molecular docking, pharmacokinetic modeling, and toxicity prediction to identify safe and potent multi-target phytochemical candidates for Type 2 Diabetes Mellitus (T2DM) management. By simultaneously targeting 17β-Hydroxysteroid Dehydrogenase (1BHS), Glucokinase (1V4S), and Maltase-Glucoamylase (3CTT), we uncovered a network of enzyme–ligand interactions that converge on the regulation of steroid metabolism, glucose phosphorylation, and carbohydrate digestion—three pivotal axes of glucose homeostasis. Among the screened compounds, Epicatechin emerged as the most promising lead, exhibiting consistent nanomolar-range docking affinities, complete compliance with major drug-likeness rules, high gastrointestinal absorption, and a broad safety margin ($LD_{50} > 2000$ mg·kg^{-1}). Its balanced pharmacological and physicochemical properties underscore the potential of small flavonoids as multitarget metabolic regulators. In contrast, larger polyphenolics such as Silymarin and Procyanidin demonstrated higher binding energies but limited oral bioavailability, highlighting the critical trade-off between potency and pharmacokinetic feasibility in phytochemical drug development. The collective results suggest that natural product scaffolds, particularly Epicatechin, can serve as templates for the rational design of next-generation antidiabetic therapeutics that integrate endocrine, enzymatic, and digestive modulation. Future experimental validation—through enzymatic inhibition assays, cellular uptake studies, and in vivo metabolic profiling- will be essential to confirm these computational predictions and translate them into clinically viable outcomes.

Abbreviations

ADME, absorption, distribution, metabolism, and excretion; CYP, cytochrome P450; DPP-4, dipeptidyl peptidase-4; GI, gastrointestinal; GLP-1 RAs, glucagon-like peptide-1 receptor agonists; GSK3β, glycogen synthase kinase-3 beta; IC_{50}, half-maximal inhibitory concentration; LD_{50}, median lethal dose; PDB, Protein Data Bank; PPAR-γ, peroxisome proliferator-activated receptor gamma; QSAR, quantitative structure–activity relationship; Ro5, Lipinski's Rule of Five; T2DM, Type 2 Diabetes Mellitus; DM, Diabetes Mellitus; 1BHS, 17β-Hydroxysteroid Dehydrogenase; 1V4S, Glucokinase; 3CTT, Maltase-Glucoamylase.

Ethics approval and consent to participate: Not applicable.

Consent for publication: Not applicable.

Data Availability Statement: The datasets generated and analyzed during the current study are available from the corresponding author on reasonable request.

Declaration of Competing Interest: The authors declare that the research was conducted in the absence of any commercial or financial relationships that could be construed as a potential conflict of interest.

References

[1] Corcoran, C., Tibb, ;, & Jacobs, F. (n.d.-a). Metformin Continuing Education Activity.

[2] Costello, R. A., Nicolas, S., & Shivkumar, A. (n.d.). Sulfonylureas Continuing Education Activity.

[3] Kocarnik, B. M., Moore, K. P., Smith, N. L., & Boyko, E. J. (2017). Weight change after initiation of oral hypoglycemic monotherapy for diabetes predicts 5-year mortality: An observational study. *Diabetes Research and Clinical Practice*, 123, 181–191. https://doi.org/10.1016/j.diabres.2016.11.025

[4] Makhoba, X. H., Viegas, C., Mosa, R. A., Viegas, F. P. D., & Pooe, O. J. (2020). Potential impact of the multi-target drug approach in the treatment of some complex diseases. *Drug Design, Development and Therapy*, 14, 3235–3249. https://doi.org/10.2147/DDDT.S257494

[5] McCreight, L. J., Bailey, C. J., & Pearson, E. R. (2016). Metformin and the gastrointestinal tract. In *Diabetologia* (Vol. 59, Issue 3, pp. 426–435). Springer Verlag. https://doi.org/10.1007/s00125-015-3844-9

[6] Mellini, M., di Muzio, E., D'Angelo, F., Baldelli, V., Ferrillo, S., Visca, P., Leoni, L., Polticelli, F., & Rampioni, G. (2019). In silico Selection and Experimental Validation of FDA-Approved Drugs as Anti-quorum Sensing Agents. *Frontiers in Microbiology*, 10. https://doi.org/10.3389/fmicb.2019.02355

[7] Mulvihill, E. E., & Drucker, D. J. (2014). Pharmacology, physiology, and mechanisms of action of dipeptidyl peptidase-4 inhibitors. In *Endocrine Reviews* (Vol. 35, Issue 6, pp. 992–1019). Endocrine Society. https://doi.org/10.1210/er.2014-1035

[8] Patil, P. J., & Shrivastava, S. K. (2014). Diabetes Mellitus: An Overview. *International Journal of Pharmaceutical Drug Analysis*, 2(7), 577–594.

[9] Roney, M., & Mohd Aluwi, M. F. F. (2024). The importance of in-silico studies in drug discovery. In *Intelligent Pharmacy* (Vol. 2, Issue 4, pp. 578–579). KeAi Publishing Communications Ltd. https://doi.org/10.1016/j.ipha.2024.01.010

[10] Siam, N. H., Snigdha, N. N., Tabasumma, N., & Parvin, I. (2024). Diabetes Mellitus and Cardiovascular Disease: Exploring Epidemiology, Pathophysiology, and Treatment Strategies. In *Reviews in Cardiovascular Medicine* (Vol. 25, Issue 12). IMR Press Limited. https://doi.org/10.31083/j.rcm2512436

[11] Vishnupriya M, Vishva N, & Vasanth A. (n.d.). Neurological Implications of Diabetes: A Comprehensive Review. *Journal of Hospital Pharmacy An Official Publication of Bureau for Health & Education Status Upliftment Hosp. Pharmacy*, 18(2), 14. http://www.journalofhospitalpharmacy.in

[12] Wang, L., Li, J., & Di, L. jun. (2022). Glycogen synthesis and beyond, a comprehensive review of GSK3 as a key regulator of metabolic pathways and a therapeutic target for treating metabolic diseases. In *Medicinal Research Reviews* (Vol. 42, Issue 2, pp. 946–982). John Wiley and Sons Inc. https://doi.org/10.1002/med.21867

[13] Wang, L., Li, J., Tang, P., Zhu, D., Tai, L., Wang, Y., Miyata, T., Woodgett, J. R., & Di, L. (2024). GSK3-β Deficiency Expands Obese Adipose Vasculature to Mitigate Metabolic Disorders. *Circulation Research*. https://doi.org/10.1161/CIRCRESAHA.124.325187

[14] Wankhede, Y. S., Khairnar, V. v., Patil, A. R., & Darekar, A. B. (2024). Drug Discovery Tools and In Silico Techniques: A Review. *International Journal of Pharmaceutical Sciences Review and Research*, 84(7). https://doi.org/10.47583/ijpsrr.2024.v84i07.009

[15] Yang DR, Wang MY, Zhang CL, & Wang Y. (2024). Endothelial dysfunction in vascular complications of diabetes: a comprehensive review of mechanisms and implications. *Frontiers in Endocrinology (Lausanne)*, 15:1359255. https://doi.org/10.3389/fendo.2024.1359255

[16] Yao, H., Zhang, A., Li, D., Wu, Y., Wang, C. Z., Wan, J. Y., & Yuan, C. S. (2024b). Comparative effectiveness of GLP-1 receptor agonists on glycaemic control, body weight, and lipid profile for type 2 diabetes: Systematic review and network meta-analysis. *BMJ*. https://doi.org/10.1136/bmj-2023-076410

[17] Zainab B., Ayaz Z., Alwahibi M. S., Khan S., Rizwana H., Soliman D. W., Alawaad A., Mehmood Abbasi A. (2020). In-silico elucidation of *Moringa oleifera* phytochemicals against diabetes mellitus. *Saudi Journal of Biological Sciences*, 27(9), 2299–2307. https://doi.org/10.1016/j.sjbs.2020.04.002